JACS
JOURNAL OF THE AMERICAN CHEMICAL SOCIETY

Communication

pubs.acs.org/JACS

Electrocatalytic Hydrogen Evolution under Acidic Aqueous Conditions and Mechanistic Studies of a Highly Stable Molecular Catalyst

Charlene Tsay and Jenny Y. Yang*

Department of Chemistry, University of California, Irvine, California 92697, United States

Supporting Information

ABSTRACT: Electrocatalytic activity of a water-soluble nickel complex, $[Ni(DHMPE)_2]^{2+}$ (DHMPE = 2-bis(di-(hydroxymethyl)phosphino)ethane), for the hydrogen evolution reaction (HER) at pH 1 is reported. The catalyst functions at a rate of $\sim 10^3$ s^{-1} (k_{obs}) with high Faradaic efficiency. Quantification of the complex before and after 18+ hours of electrolysis reveals negligible decomposition under catalytic conditions. Although highly acidic conditions are common in electrolytic cells, this is a rare example of a homogeneous catalyst for HER that functions with high stability at low pH. The stability of the compound and proposed catalytic intermediates enabled detailed mechanistic studies. The thermodynamic parameters governing electron and proton transfer were used to determine the appropriate reductants and acids to access the catalytic cycle in a stepwise fashion, permitting direct spectroscopic identification of intermediates. These studies support a mechanism for proton reduction that proceeds through two-electron reduction of the nickel(II) complex, protonation to generate $[HNi(DHMPE)_2]^+$, and further protonation to initiate hydrogen bond formation.

Hydrogen is a valuable commodity as a fuel and reductant that is predominately produced from natural gas and other fossil fuel sources with concomitant generation of carbon dioxide.[1] An alternative approach would utilize energy from renewable sources in an aqueous electrolytic cell to produce hydrogen and oxygen from water.[2−6] The resulting hydrogen would be carbon-neutral and free of CO impurities, which can poison hydrogen oxidation catalysts found in fuel cells.[7] As a result, there is significant interest in the development of stable and well-defined molecular electrocatalysts for the production of hydrogen from water.[8−11]

Isolation of hydrogen from oxygen gas in electrolytic cells requires separation of the cathodic and anodic chambers by an ion-conductive membrane. Proton exchange membranes are most frequently used and are most effective under highly acidic conditions.[12] Although there are an increasing number of earth-abundant molecular electrocatalysts with activity for the hydrogen evolution reaction (HER) in partially or fully aqueous conditions,[9,13−19] very few function under acidic aqueous conditions.[20−23] Of the latter, there is evidence that some are precatalysts that generate the active heterogeneous catalyst upon reduction.[24,25]

In the course of our studies on water-soluble transition metal hydrides, we recently reported the nickel diphosphine complex, $[Ni(DHMPE)_2][BF_4]_2$ (**1**), shown in Chart 1.[26] We found **1** to

Chart 1

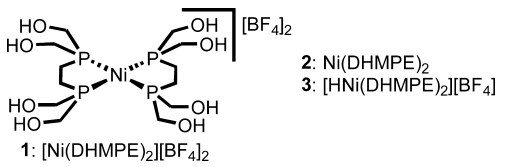

be stable under acidic conditions. Specifically, a 1 mM solution of **1** in 0.1 M H_2SO_4 (pH 1) was monitored by $^{31}P\{^1H\}$ NMR spectroscopy; integration of the singlet $^{31}P\{^1H\}$ NMR resonance at 65.2 ppm against a H_3PO_4 capillary confirmed no observable decomposition after 72 h at room temperature (Figure S10).

We investigated the electrocatalytic activity of **1** toward proton reduction at pH 1 and found it to be very active and exceptionally stable, with a high rate of turnover at a modest overpotential. While mechanistic insight into hydrogen bond formation is essential to understanding catalytic design principles, it has been challenging to establish in most previously reported HER catalysts. For this catalyst, however, we capitalize on the independent synthesis of diamagnetic intermediates and their thermochemical properties to interrogate the catalytic mechanism using appropriate electron and proton transfer reagents. As a result, we directly observe spectroscopic evidence of a viable catalytic pathway involving hydrogen bond formation through heterocoupling. The proposed mechanism also suggests possible avenues for modifying the catalyst to improve activity.

Cyclic voltammograms (CVs) of **1** at pH 1 exhibit an irreversible reduction at −0.53 V vs SHE at scan rates up to 39 000 mV/s (shown in Figure 1 up to 1000 mV/s). Complex **1** undergoes a similar two-electron irreversible reduction in acetonitrile.[26] Although this reduction is not electrochemically reversible, the corresponding Ni(0) complex (**2**) is isolable and stable. We attribute the electrochemical irreversibility to hydrogen bonding interactions between the DHMPE ligands on each nickel, which are disrupted in the geometric change from square planar in the Ni(II) complex to tetrahedral in the Ni(0) complex. These intramolecular hydrogen bonds are observed in the solid-state structure of **1**.[26]

Received: June 7, 2016
Published: July 14, 2016

DOI: 10.1021/jacs.6b05851
J. Am. Chem. Soc. 2016, 138, 14174−14177

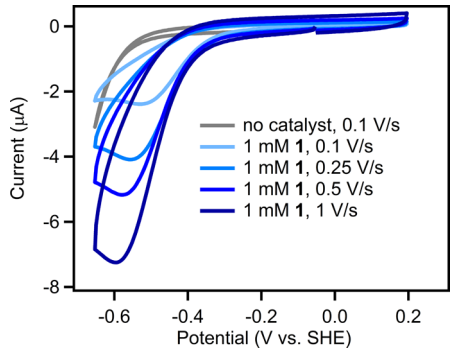

Figure 1. CVs of 1 mM $[Ni(DHMPE)_2][BF_4]_2$ (**1**) in 0.1 M H_2SO_4 at various scan rates (blue traces). The gray trace displays the background reduction with the working electrode (glassy carbon) under the same conditions.

To ascertain whether the reductive wave in the CVs corresponds to catalytic proton reduction at pH 1, controlled potential electrolyses was performed. The electrolyses were performed in a glass vessel with the counter electrode separated from the bulk solution by a fine fritted glass disc (Figure S1). Carbon foam cylinders were used for the working and counter electrodes, and an aqueous Ag/AgCl (saturated KCl) electrode was used as the reference.

The cumulative current passed over an 18.3 h electrolysis at −0.60 V vs SHE in a 1 mM solution of **1** at pH 1 is shown in Figure 2 (blue trace). An electrolysis of an equivalent pH 1

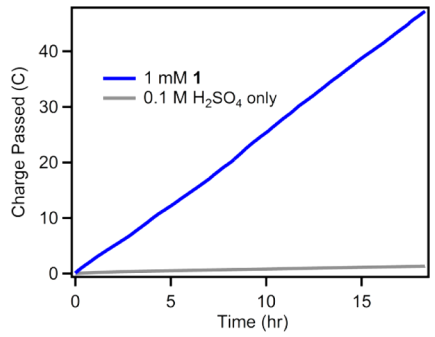

Figure 2. Accumulation of charge vs time in the controlled potential electrolysis of a 1 mM solution of **1** at pH 1 over 18.3 h (66 000 s) at −0.60 V vs SHE (blue) and equivalent electrolysis under the same conditions in the absence of **1** (grey).

solution without catalyst was performed to quantify the small amount of background proton reduction at the glassy carbon electrode (Figure 2, gray trace). The current measured over time under both conditions is shown in Figures S2 and S3.

The quantity of hydrogen evolved was measured using gas chromatography. The calculated Faradaic yield ranged from 92 to 105% after correcting for background hydrogen formation at the glassy carbon electrode and H_2 loss through cell leakage during the 18.3 h electrolysis (details in Figure S7 and Table S1). The total amount of hydrogen generated corresponds to between 7 and 9 equiv of hydrogen with respect to **1**, confirming its catalytic activity. The linear increase in charge passed as a function of time (Figure 2, blue) indicates the stability of the catalyst over the electrolysis, which was corroborated by analyzing the pre- and post-electrolysis solutions. Both exhibit only the $^{31}P\{^1H\}$ NMR resonance for **1**, and integration against a H_3PO_4 capillary standard confirmed quantitative retention of the catalyst (Figure S4).

A mercury pool was included at the bottom of the electrolytic cell during the electrolysis to amalgamate any potential heterogeneous nickel particles and ensure that catalysis was occurring homogeneously.[27] Additionally, after electrolysis, the working electrode was rinsed with water and placed into a fresh 0.1 M H_2SO_4 solution.[27] No current above background was observed, demonstrating the absence of any active catalyst absorbed or deposited onto the electrode surface (Figure S5).

For conditions where electrocatalytic activity is fast and irreversible with no catalyst decomposition or product inhibition, "pure kinetic" conditions can be achieved in CV studies. Under these conditions, the concentration profile of the resting and active catalysts is maintained in the electrode diffusion layer. If the substrate is in sufficient excess that consumption is negligible (catalyst is under pseudo-first-order kinetic conditions), the resulting catalytic current will form a scan-rate-independent S-shaped current−potential response.[28,29] Under these conditions, the maximum current (i_{cat}) can be used to derive the observed rate constant for the electrocatalyst according to eq 1, where n is the number of electrons per catalytic cycle, F is Faraday's constant, A is the electrochemically active surface area of the electrode in cm^2, [cat] is the concentration of the catalyst in M, D is the diffusion coefficient in $cm^2 \cdot s^{-1}$, and k_{obs} is the observed rate constant in s^{-1}:[30−32]

$$k_{obs} = \left(\frac{i_{cat}}{nFA[cat]}\right)^2 D^{-1} \quad (1)$$

Since the substrate concentration ($[H^+]$) is defined at pH 1, we achieved pseudo-first-order conditions and pure kinetic conditions by decreasing the catalyst concentration and increasing the scan rate, respectively. The former increases the concentration of substrate relative to the catalyst, and the latter decreases the volume of the diffusion layer. At 0.1 mM of **1** at pH 1, the catalytic current (i_{cat}) approaches a scan-rate-independent value of 2.2×10^{-5} A around 39 V/s (Figure S11). The reductive current (i_p) under noncatalytic conditions is often used to account for D and A in complexes with reversible redox couples. Since the reduction of **1** is irreversible and catalytic at pH 1, D and A were determined using alternative methods. The diffusion constant of **1** in water was measured to be 4.88×10^{-6} cm^2/s using a DOSY ^1H NMR experiment (Figure S6).[33] The electrochemically active surface area of the glassy carbon electrode was determined to be 0.012 cm^2 via chronoamperometry measurements of an $Fe(C_5H_5)_2$ solution (Figure S9 and Table S2).[34] These values, combined with the scan-rate-independent catalytic current, result in an observed rate (turnover frequency) of 1850 s^{-1} for **1** at pH 1.

The operating potential of the catalyst based on the potential at half the maximum catalytic current ($E_{cat/2}$)[35] is −0.54 V vs SHE, representing a modest overpotential of ∼480 mV. We note that to maximize product formation and increase the accuracy of the Faradaic yield, electrolysis was performed at the potential of maximum current (i_{cat}) rather than $E_{cat/2}$.

The fast rate of catalysis precluded our efforts to detect any intermediates in the catalytic cycle under aqueous conditions at pH 1. To gain insight into the mechanism of H_2 formation, we investigated the stepwise catalytic mechanism of hydrogen production under noncatalytic conditions using stoichiometric reagents, as shown in Figure 3. This study was facilitated by prior independent synthesis and characterization of the diamagnetic

DOI: 10.1021/jacs.6b05851
J. Am. Chem. Soc. 2016, 138, 14174−14177

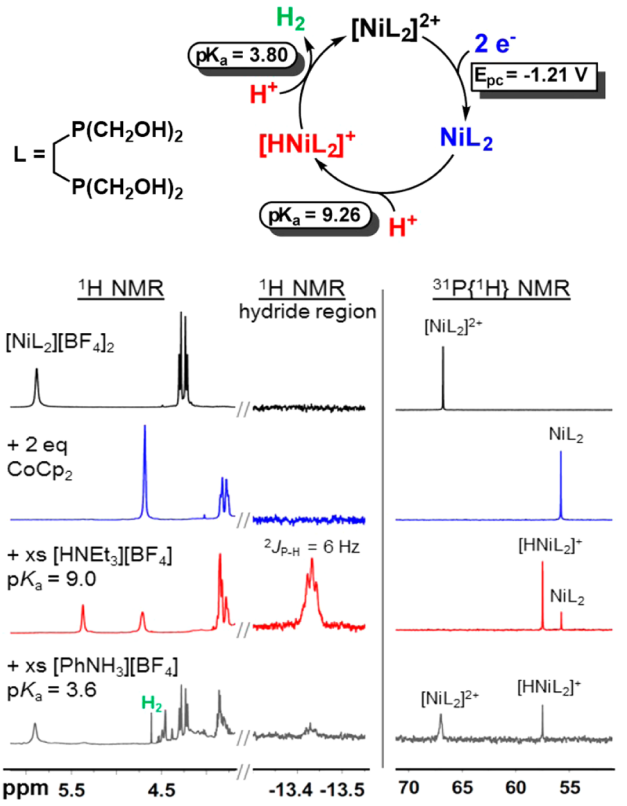

Figure 3. (Top) Proposed catalytic cycle for hydrogen evolution. The value of E_{pc} (vs $Fe(C_5H_5)_2^{0/+}$) shown in the catalytic cycle is in acetonitrile, and pK_a values are in DMSO. (Bottom) ^{1}H and ^{31}P{^{1}H} NMR in DMSO-d_6 upon addition of electron or proton transfer reagents, with identification of proposed intermediates.

$Ni(DHMPE)_2$ (**2**) and $[HNi(DHMPE)_2][BF_4]$ (**3**) complexes, which are observable by ^{1}H and ^{31}P{^{1}H} NMR spectroscopy.[26] Thermochemical properties of **1**–**3** were used to identify appropriate stoichiometric reagents for electron and proton transfer. To control proton delivery and enable identification of the hydride peak in the ^{1}H NMR spectra, these studies were carried out in the aprotic solvents CD_3CN and DMSO-d_6.

Compound **1** undergoes a two-electron reduction at approximately −1.21 V vs the $Fe(C_5H_5)_2^{0/+}$ couple in acetonitrile,[26] confirming our choice to use 2 equiv of $Co(C_5H_5)_2$ (−1.34 V vs $Fe(C_5H_5)_2^{0/+}$; see Figure S8) to synthesize the Ni(0) complex (**2**) by chemical reduction. ^{1}H and ^{31}P{^{1}H} NMR spectra of the isolated Ni(0) (**2**) complex are shown in Figure 3.

The pK_a of $[HNi(DHMPE)_2]^+$ (**3**) is 9.26 in DMSO,[26] which dictates the strength of the acid needed to protonate **2** to generate the hydride **3** while inhibiting additional protonation to form H_2. Accordingly, addition of excess triethylammonium tetrafluoroborate (pK_a 9.0 in DMSO)[36] results in an equilibrium between **2** and protonated **3**, also shown in Figure 3.

The hydricity ($\Delta G^\circ_{H^-}$, eq 2) of $[HNi(DHMPE)_2]^+$ (**3**) quantifies the acid strength needed to thermodynamically favor protonation of the hydride to release H_2 according to eq 3, where $\Delta G^\circ_{H_2}$ is the free energy of H_2 heterolysis (60.7 kcal/mol in DMSO).[37] The $\Delta G^\circ_{H^-}$ of **3** is 55.5 kcal/mol in DMSO,[26] indicating that acids with a pK_a < 3.80 will result in a negative free energy for hydrogen bond formation. Addition of anilinium tetrafluoroborate (pK_a 3.6 in DMSO)[36] results in hydrogen evolution, which is observed in the ^{1}H NMR spectrum with concomitant re-formation of the Ni(II) resting catalyst (Figure 3).

$$[HNi(DHMPE)_2]^+ \rightleftharpoons [Ni(DHMPE)_2]^{2+} + H^- \quad \Delta G^\circ_{H^-} \tag{2}$$

$$[HNi(DHMPE)_2]^+ + [HB]^+ \rightleftharpoons [Ni(DHMPE)_2]^{2+} + B + H_2 \tag{3}$$

$$\Delta G^\circ \text{ (kcal/mol)} = \Delta G^\circ_{H^-} + 1.37 \times pK_{a(HB)} - \Delta G^\circ_{H_2}$$

The mechanistic study of this catalyst using stoichiometric reagents demonstrates a chemically accessible route for H_2 formation by protonation of a metal hydride but does not preclude other pathways. A number of mechanisms have been proposed for H_2 evolution by molecular catalysts. In general, they differ on whether bond formation proceeds through hetero- or homocoupling or in the specific sequence of electron and proton transfers.

Hydrogen bond formation via homocoupling proceeds either through reductive elimination or the bimolecular reaction of two metal hydride complexes, and has been proposed for cobalt dimethylglyoxine catalysts.[38−41] To examine this possibility, **3** was isolated in both DMSO and water for 3 days at room temperature (see Figures S14 and S15, respectively). No appreciable H_2 evolution or decrease in the concentration of nickel hydride (through use of an internal standard) was observed by ^{1}H and ^{31}P{^{1}H} NMR spectroscopy, demonstrating that **3** is stable with respect to bimolecular H_2 formation.

Another possible catalytic route is reduction of the incipiently generated $[HNi(II)(DHMPE)_2]^+$ (**3**) under electrocatalytic conditions. The resulting reduced Ni(I) hydride could potentially be competent for catalytic H_2 formation through a hetero- or homocoupling pathway; both routes have been proposed for molecular cobalt-based HER electrocatalysts.[40−43] However, the CV of **3** in water establishes that it is reduced at a potential ∼400 mV more negative than **1** (see Figures S13 and S12) and is inaccessible under electrocatalytic conditions.

Recent studies on closely related nickel bis(diphosphine)[44,45] catalysts in organic solvents indicate two mechanisms for hydrogen evolution that differ in the order of proton and electron transfer. The proposed pathways are (1) alternating electron and proton transfer or (2) two successive reductions followed by two protonation steps. Since reduction of **1** is a $2e^-$ event, we believe the mechanism of **1** is closer to the latter, which is supported by the catalytic pathway outlined in Figure 3.

The proposed mechanism suggests an avenue for decreasing the overpotential required for catalysis. The most straightforward modification would be to increase the electron-withdrawing nature of the ligand environment to shift the reduction potential to more positive values, resulting in a decrease in overpotential at pH 1. However, the hydricity is dictated by the reduction potential of the complex (and to a lesser extent pK_a of the metal hydride).[37,46] Therefore, this modification would also decrease the hydricity of the corresponding metal hydride intermediate. Since protonation to form hydrogen is dependent on hydricity (eq 3), it is reasonable to suspect that this type of catalyst modification would have an unfavorable impact on the hydrogen bond formation step in the catalytic cycle. Our study indicates that nickel hydride intermediate **3** is already appropriately hydridic to favor protonation at pH 1. However, we propose another possible route to shifting the catalytic onset potential to more positive values without significantly affecting the reductive

DOI: 10.1021/jacs.6b05851
J. Am. Chem. Soc. 2016, 138, 14174−14177

properties of the nickel complex. Since electrochemical reduction of **1** is irreversible, the thermodynamic reduction potential is positive of the observed potential. The irreversibility of the $2e^-$ reduction is likely due to intramolecular hydrogen bonding between the two DHMPE ligands. Therefore, we are exploring ligand modifications that would maintain a similar electronic structure at the metal while eliminating the source of electrochemical irreversibility. This would permit access to an energetically similar metal hydride intermediate at more positive potentials, leading to a reduction in overpotential without a corresponding decrease in rate.

In conclusion, we report a highly stable catalyst for the electrocatalytic reduction of protons to hydrogen. The catalyst functions at high rates at a modest overpotential under acidic conditions, which are most applicable to current electrolytic cells for solar fuels. Furthermore, the stability of the complex and potential catalytic intermediates, along with thermochemical parameters, was used to interrogate the catalytic pathway in detail. The mechanistic insight derived from this study is critical to understanding hydrogen bond formation and permits the rational design of new catalysts with improved activity.

■ ASSOCIATED CONTENT

Supporting Information

The Supporting Information is available free of charge on the ACS Publications website at DOI: 10.1021/jacs.6b05851.

Experimental details, compound characterization, controlled potential electrolysis data and analysis, GC and other calibrations (PDF)

■ AUTHOR INFORMATION

Corresponding Author

*j.yang@uci.edu

Notes

The authors declare no competing financial interest.

■ ACKNOWLEDGMENTS

This material is based on work supported by the U.S. Department of Energy, Office of Science, Office of Basic Energy Sciences, under Award No. DE-SC0012150.

■ REFERENCES

(1) Ogden, J. M. *Annual Review of Energy and the Environment* **1999**, *24*, 227.
(2) Turner, J. A. *Science* **2004**, *305*, 972.
(3) Bard, A. J.; Fox, M. A. *Acc. Chem. Res.* **1995**, *28*, 141.
(4) Graetzel, M. *Acc. Chem. Res.* **1981**, *14*, 376.
(5) Lewis, N. S. *Science* **2007**, *315*, 798.
(6) Crabtree, G. W.; Dresselhaus, M. S. *MRS Bull.* **2008**, *33*, 421.
(7) Wee, J.-H.; Lee, K.-Y. *J. Power Sources* **2006**, *157*, 128.
(8) Lewis, N. S.; Nocera, D. G. *Proc. Natl. Acad. Sci. U. S. A.* **2006**, *103*, 15729.
(9) Thoi, V. S.; Sun, Y.; Long, J. R.; Chang, C. *Chem. Soc. Rev.* **2013**, *42*, 2388 and references therein.
(10) Tran, P. D.; Artero, V.; Fontecave, M. *Energy Environ. Sci.* **2010**, *3*, 727.
(11) Artero, V.; Fontecave, M. *Coord. Chem. Rev.* **2005**, *249*, 1518.
(12) Li, W.; Sheehan, S. W.; He, D.; He, Y.; Yao, X.; Grimm, R. L.; Brudvig, G. W.; Wang, D. *Angew. Chem., Int. Ed.* **2015**, *54*, 11428.
(13) Kandemir, B.; Kubie, L.; Guo, Y.; Sheldon, B.; Bren, K. L. *Inorg. Chem.* **2016**, *55*, 1355.
(14) Kleingardner, J. G.; Kandemir, B.; Bren, K. L. *J. Am. Chem. Soc.* **2014**, *136*, 4.
(15) Zee, D. Z.; Chantarojsiri, T.; Long, J. R.; Chang, C. *Acc. Chem. Res.* **2015**, *48*, 2027.
(16) Nguyen, A. D.; Rail, M. D.; Shanmugam, M.; Fettinger, J. C.; Berben, L. A. *Inorg. Chem.* **2013**, *52*, 12847.
(17) Wang, Z.-Q.; Tang, L.-Z.; Zhang, Y.-X.; Zhan, S.-Z.; Ye, J.-S. *J. Power Sources* **2015**, *287*, 50.
(18) Eckenhoff, W. T.; Brennessel, W. W.; Eisenberg, R. *Inorg. Chem.* **2014**, *53*, 9860.
(19) Halter, D. P.; Heinemann, F. W.; Bachmann, J.; Meyer, K. *Nature* **2016**, *530*, 317.
(20) Dutta, A.; Lense, S.; Hou, J.; Engelhard, M. H.; Roberts, J. A. S.; Shaw, W. J. *J. Am. Chem. Soc.* **2013**, *135*, 18490.
(21) Dutta, A.; DuBois, D. L.; Roberts, J. A. S.; Shaw, W. *Proc. Natl. Acad. Sci. U. S. A.* **2014**, *111*, 16286.
(22) Kellett, R. M.; Spiro, T. G. *Inorg. Chem.* **1985**, *24*, 2373.
(23) Abdel-Hamid, R.; El-Sagher, H. M.; Abdel-Mawgoud, A. M.; Nafady, A. *Polyhedron* **1998**, *17*, 4535.
(24) Luca, O. R.; Konezny, S. J.; Blakemore, J. D.; Colosi, D. M.; Saha, S.; Brudvig, G. W.; Batista, V. S.; Crabtree, R. H. *New J. Chem.* **2012**, *36*, 1149.
(25) Kaeffer, N.; Morozan, A.; Fize, J.; Martinez, E.; Guetaz, L.; Artero, V. *ACS Catal.* **2016**, *6*, 3727.
(26) Tsay, C.; Livesay, B. N.; Ruelas, S.; Yang, J. Y. *J. Am. Chem. Soc.* **2015**, *137*, 14114.
(27) Artero, V.; Fontecave, M. *Chem. Soc. Rev.* **2013**, *42*, 2338.
(28) Artero, V.; Saveant, J.-M. *Energy Environ. Sci.* **2014**, *7*, 3808.
(29) Savéant, J. M.; Su, K. B. *J. Electroanal. Chem. Interfacial Electrochem.* **1984**, *171*, 341.
(30) Nicholson, R. S.; Shain, I. *Anal. Chem.* **1964**, *36*, 706.
(31) Saveant, J. M.; Vianello, E. *Electrochim. Acta* **1965**, *10*, 905.
(32) Longmuir, I. S. *Advances in Polarography: Proceedings of the Second International Congress Held at Cambridge, 1959*; Symposium Publications Division; Pergamon Press, 1960.
(33) Pool, D. H.; Stewart, M. P.; O'Hagan, M.; Shaw, W. J.; Roberts, J. A. S.; Bullock, R. M.; DuBois, D. L. *Proc. Natl. Acad. Sci. U. S. A.* **2012**, *109*, 15634.
(34) Kadish, K. M.; Ding, J. Q.; Malinski, T. *Anal. Chem.* **1984**, *56*, 1741.
(35) Appel, A. M.; Helm, M. L. *ACS Catal.* **2014**, *4*, 630.
(36) Kolthoff, I. M.; Chantooni, M. K.; Bhowmik, S. *J. Am. Chem. Soc.* **1968**, *90*, 23.
(37) Wayner, D. D. M.; Parker, V. D. *Acc. Chem. Res.* **1993**, *26*, 287.
(38) Hu, X.; Brunschwig, B. S.; Peters, J. C. *J. Am. Chem. Soc.* **2007**, *129*, 8988.
(39) Dempsey, J. L.; Brunschwig, B. S.; Winkler, J. R.; Gray, H. B. *Acc. Chem. Res.* **2009**, *42*, 1995.
(40) Solis, B. H.; Hammes-Schiffer, S. *Inorg. Chem.* **2011**, *50*, 11252.
(41) Dempsey, J. L.; Winkler, J. R.; Gray, H. B. *J. Am. Chem. Soc.* **2010**, *132*, 16774.
(42) Muckerman, J. T.; Fujita, E. *Chem. Commun.* **2011**, *47*, 12456.
(43) Costentin, C.; Dridi, H.; Savéant, J.-M. *J. Am. Chem. Soc.* **2014**, *136*, 13727.
(44) Rountree, E. S.; Dempsey, J. L. *J. Am. Chem. Soc.* **2015**, *137*, 13371.
(45) Wiedner, E. S.; Brown, H. J. S.; Helm, M. L. *J. Am. Chem. Soc.* **2016**, *138*, 604.
(46) Berning, D. E.; Noll, B. C.; DuBois, D. L. *J. Am. Chem. Soc.* **1999**, *121*, 11432.

DOI: 10.1021/jacs.6b05851
J. Am. Chem. Soc. 2016, 138, 14174−14177